

# CU Boulder MagNet Challenge Final Report

Bailey Sauter\*, Skye Reese\*, Shivangi Sinha\*,

\*Ph.D. Students

Colorado Power Electronics Center

University of Colorado Boulder

Email: {basa4247, skre2597, shsi3480}@colorado.edu

**Abstract**—This report summarizes the work of the University of Colorado at Boulder (CU-Boulder) team on the IEEE PELS MagNet challenge to predict core loss in magnetic components. This report presents a novel approach that integrates an existing equation-based core loss algorithm based on Steinmetz parameters with a simple random forest regression model to provide greater accuracy in core loss predictions without incurring significant computational costs. This hybrid model uses the equation-based model as a starting point and attempts to predict and correct the error through a multiplicative correction coefficient. The regression that produces the correction coefficient is trained using the MagNet database of experimentally measured core loss data, which includes a wide variety of materials and operating conditions [1]. Results for the ten original MagNet challenge materials are provided alongside test results on the five new, unidentified materials (labeled as A-E). Results across all materials showed an average 4x reduction in percent error estimating volumetric core loss.

## I. INTRODUCTION

The MagNet [1] database offers a large amount of experimentally measured core loss samples available for validation and training. This enables a more in-depth look into alternative data-driven core loss modeling approaches that expand on existing, equation-based models like GSE [2] and iGSE [3]. Recent work has explored the use of neural networks, of both deep and convolutional types, for this application [4]–[6]. However, neural networks can be quite complex to set up and train and can require significant computational resources along with large input vectors.

This report introduces a method that improves upon the previously developed equation-based models by adding a relatively simple machine learning (ML) based regression with easy-to-obtain input features and using it in a hybrid model to predict a multiplicative correction factor for the iGSE algorithm. Specifically, a random forest regression is chosen for this task due to its simplicity, accuracy, and resistance to overfitting [7]. The result is a simple, computationally inexpensive, hybrid model that provides significant improvements

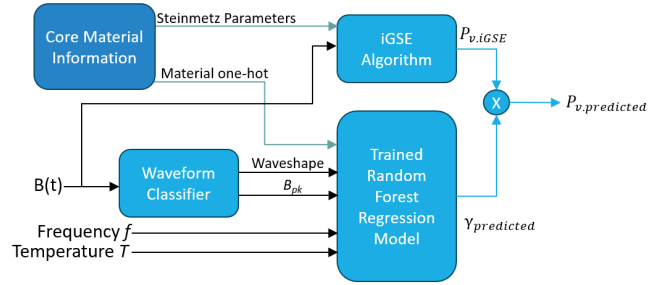


Figure 1: A flowchart illustrating the structure of the CU-Boulder hybrid model: core loss predictions obtained using the iGSE algorithm are corrected via a multiplicative correction factor  $\gamma_{predicted}$  generated by a regression trained on the core loss data samples in the MagNet database.

over standard equation-based approaches. A flowchart of the proposed hybrid model is shown in Fig. 1.

The report is organized as follows. Data pre-processing aimed at waveform classification and optimization of Steinmetz parameters for sinusoidal waveforms is addressed in Section II. Section III summarizes the results of core loss prediction on the database using existing, equation-based methods. Section IV presents the results of the novel hybrid model, its improvement over existing standard algorithms, and its potential for use in the power electronics design process. Section V summarizes the results and concludes the report.

## II. DATA PRE-PROCESSING

The database used to train and evaluate the model in this report is the database of core loss samples provided by the research group at Princeton University [1]. The initial data is made up of 186,757 core loss samples of ten ferrite materials. The materials are all commonly available and range in designed frequency from below 100 kHz to an upper bound of 2 MHz. The tested operating frequencies within the database range from below 50 kHz to greater than 600 kHz. The sampled temperatures range from 25°C to 100°C. The database includes sinusoidal, triangular, and trapezoidal flux-density waveforms, of varying slopes and duty cycles.

After the initial model was designed and trained using the aforementioned dataset, limited data for five additional materials, labeled A-E and of unknown identity and type,

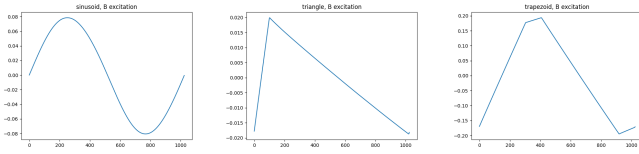


Figure 2: An example of sinusoidal, triangular, and trapezoidal waveform types respectively, all classified correctly by the algorithm.

was provided and incorporated into the model’s training. This limited data included 17,782 new samples that could be used in training, with an additional group of samples (core loss not provided) also present for final scoring of the model performance within the MagNet challenge.

#### A. Waveform Classification

In order to gain more information about the core loss samples in the database, an algorithm was implemented to classify the samples in the database based on the waveshape of their flux-density waveforms. All the flux-density waveforms in the database of samples [1] fall into one of three categories: sinusoidal, trapezoidal, or triangular waveshapes, which are the most common flux-density waveforms in switched-mode power converters. Therefore, these are the categories used and referenced in the rest of the report.

The classification of sinusoidal waveforms is performed by first taking the Fourier transform and analyzing its power spectral density. A power spectral density value above .499 indicates a sinusoidal waveform. For non-sinusoidal waveshapes, the derivative of the waveform is taken. The waveform is split up into segments based on when the slope changes. The number of segments is analyzed in order to differentiate between triangular and trapezoidal waveforms (2 segments for a triangular waveform, 4 segments for a trapezoidal waveform). Examples of each category of waveshape are shown in Fig. 2.

A flux-density waveform classification accuracy of >99% was measured on the limited dataset (materials A-E). Wave-shape information was not provided on the initial, larger dataset, but accuracy can be assumed to be similar based on visual inspection of random samples and given that the waveshapes should not depend on the material.

#### B. Optimization of Steinmetz Parameters for Sinusoidal Data

The Generalized Steinmetz Equation (GSE), Eq. (1), attempts to predict volumetric core loss  $P_v$  in  $[W/m^3]$  (with sinusoidal excitation) using a set of simple parameters for a single core material regardless of temperature, excitation, and frequency [2].

$$P_v = k \cdot f^\alpha \cdot B_{pk}^\beta \quad (1)$$

The iGSE core loss algorithm [3] improves on Eq. (1) by breaking up waveforms into smaller subsections but uses the same input parameters. In reality, Steinmetz parameters vary based on the operating conditions and the accuracy of datasheet measurements. This introduces significant errors when selecting the Steinmetz parameters from arbitrary operating conditions in the datasheet. Given the high volume of

Model Size	774 MB (.joblib file)
Number of Parameters	100 estimators (hyperparameters incl. in text)

Table I: Regression model information

core loss samples available in the database [1], the optimal Steinmetz parameters that minimize the error in the GSE core loss calculation are found numerically, giving the ML model a starting point with a higher accuracy than hand-calculated Steinmetz parameters from a datasheet. Only samples with sinusoidal flux-density waveforms are used in this optimization because the GSE technique is explicitly designed for only sinusoidal excitation waveforms. To optimize the Steinmetz parameters, the log of Eq. 1 is taken and an Ordinary Least Squares (OLS) model is used to solve the multiple linear regression for optimal values of  $k$ ,  $\alpha$ , and  $\beta$  for each material in the database. The solver is limited by the constraints  $1.6 \leq \alpha \leq 2.0$  and  $2.3 \leq \beta \leq 2.7$ , a reasonable range of standard Steinmetz parameters, so that the GSE fits are similar across the materials. These parameters are used as an input to the equation-based model [3] in the following sections.

### III. RESULTS FOR EQUATION-BASED MODELS

After the classification of samples by waveshape and the optimization of Steinmetz parameters, initial results were generated by the GSE [2] and iGSE [3] core loss models. The mean absolute error (%) for both approaches can be seen across various materials in Table II. As expected, Table II shows that iGSE offers more accurate results than GSE and is therefore used as the starting point for the machine-learning (ML) based correction. To better understand the dataset and under what conditions the errors in existing core loss models are largest in magnitude, the error data seen in Table II for the iGSE algorithm is displayed on a heatmap in Fig. 4 plotted against the frequency and excitation magnitude with the number of points at that operating condition shown via the size of the plotted circle. The heatmaps included in the report are only based on the initial training data that is complete (10 known materials). It should be noted that in order for the heatmap to be readable, similar frequency and flux-density values are grouped together and have their absolute percent error averaged and displayed at one point.

### IV. HYBRID MODEL AND RESULTS

The structure of the hybrid model proposed in this report is shown in Fig. 1. Errors in core loss predictions obtained using the iGSE algorithm are corrected via a multiplicative correction factor  $\gamma_{predicted}$  generated by a regression trained on the core loss samples in the MagNet database [1]. The use of one-hot encoding of the material enables the use of a single model for all materials. This optimizes usability and space while improving model versatility to allow for good performance on new materials not included in the training dataset [8].

### A. Hybrid Model Structure

The regression model used in the machine learning portion of the hybrid model shown in Fig. 1 is a random forest regression model implemented using the scikit learn ensemble package in Python [9]. Random forest regression models are made up of an ensemble of decision trees [10]. Decision trees make predictions using a series of splits in the training data that are based on a sample's value of a given feature. Each decision tree is trained on a random subset (with replacement) of the training data. The resulting prediction of the random forest model is an average of the predictions of the trees that make up the ensemble. The decision tree structure of each estimator inherently captures relationships between variables and gives outlier points less influence over the model. Meanwhile, the ensemble nature of the model reduces its susceptibility to overfitting during training. These advantages make a random forest regression particularly suitable for the task of core loss estimation, which has been shown to be highly nonlinear, and not easily predictable via physics-based explanations.

The machine learning portion of the hybrid model uses the results from Section III as a starting point. A correction factor,  $\gamma$ , where

$$\gamma = P_{v.true}/P_{v.iGSE} \quad (2)$$

is calculated for each sample. This is used as the target output variable  $y$  in the training of the random forest regression model. The model was trained on 80% of the available samples and tested on the remaining 20% (of 204,539 total core loss samples across the fifteen materials). Within the training set, 10,000 samples were taken (with replacement) from each of the fifteen material categories. This method prevents overfitting to materials with more samples taken and improves performance on the new, unknown materials. The features used as inputs for the model are one-hot encoding of the material, the Steinmetz parameters of that material, temperature, peak flux density, frequency, and a one-hot encoding of the waveshapes as classified in Section II. The peak flux density is defined as

$$B_{pk} = \frac{\max(B) - \min(B)}{2} \quad (3)$$

where  $B$  is the flux density waveform of the given data sample. Features were normalized and standardized to mitigate magnitude variation before training.

After the model is trained, it is used to predict  $\gamma_{predicted}$  for the test set, which is then used to calculate the predicted  $P_v$ ,

$$P_{v.predicted} = \gamma_{predicted} \cdot P_{v.iGSE} \quad (4)$$

as shown in Fig. 1. The absolute percent errors are then calculated and compared with the results of Section III.

Table I shows the size of the model (used for all fifteen materials) after being saved as a .joblib file for future use. In the random forest regression, the hyperparameters used are  $n_{estimators} = 100$  (the number of trees in the ensemble) and  $depth_{max} = 30$  (maximum depth of each tree). Limiting the maximum depth of the trees helps prevent overfitting of the

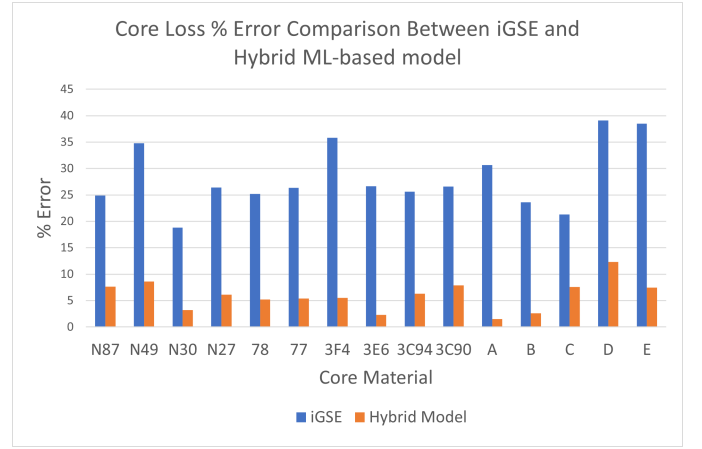


Figure 3: Histogram comparing the mean core loss % error across the 15 tested materials using the iGSE method and using the hybrid model.

model to the training data. A higher number of estimators has the potential to increase the accuracy of the model on more complex data, but, in this case, performance was found to plateau at  $n_{estimators} = 100$ . Mean squared error was used as the split criterion during the training of the decision trees.

### B. Hybrid Model Results on Test Dataset

The results of the hybrid model are presented in Tables II and III (average and 95th percentile, respectively). They show a marked improvement in accuracy compared to the equation-based models. Across all materials, the mean absolute percent error is 4x less than what it was using only the iGSE method.

A histogram comparing the results of the core loss prediction algorithm to the conventional iGSE algorithm across the ten different materials present in the dataset is shown in Fig. 3. In addition, Fig. 5 is a heatmap showing the percent error in core loss predictions generated by the hybrid model across all materials. This offers a direct comparison to Fig. 4. It can be seen that the hybrid model reduces the overall error in core loss prediction minimizes the concentration of errors at certain operating conditions. This indicates that the model is more reliably accurate across the wide variety of operating conditions present in the dataset.

Table IV is a table of the hybrid model results separated by waveshape. In all cases, across material and waveshape, the hybrid model reduces error from the iGSE model. Most flux density waveforms in power electronic circuits are non-sinusoidal. Therefore, this table demonstrates the usefulness of the proposed model's versatility across operating conditions.

In summary, the model performance on the test dataset validates the use of the hybrid model to predict core losses in switched-mode power converters. Large improvements are seen across a wide variety of materials, operating conditions, and waveshapes, demonstrating that the model is not limited to specific use cases but has the potential to serve as an effective general model for core loss. The model's performance on new ferrite materials not included in the training set demonstrates its versatility and is reported in a paper to be presented at IEEE APEC 2024 [8].

Table IV: Mean Absolute Percent Error of Models by Material, Separated by Waveshape Type

Table II: Mean Absolute Percent Error of Models by Material

Material	GSE Error [%]	iGSE Error [%]	Hybrid Model Error [%]
N87	29.13	24.93	7.62
N49	22.49	34.81	8.63
N30	26.33	18.81	3.20
N27	30.32	26.46	6.10
78	30.98	25.20	5.28
77	31.85	26.35	5.41
3F4	17.24	35.84	5.56
3E6	25.52	26.63	2.38
3C94	30.82	25.58	6.36
3C90	31.32	26.62	7.90
A	36.65	30.68	11.51
B	29.68	23.63	2.66
C	30.25	21.28	7.62
D	39.38	39.09	12.33
E	40.38	38.46	7.46

Table III: 95th percentile Absolute % Error of Models by Material

Material	GSE 95th Error [%]	iGSE 95th Error [%]	Hybrid Model 95th Error [%]
N87	70.21	57.06	27.80
N49	91.91	89.78	31.67
N30	72.46	48.49	9.71
N27	72.11	59.81	21.96
78	73.84	60.18	17.10
77	74.31	62.55	18.51
3F4	89.31	86.61	18.10
3E6	79.71	81.24	7.39
3C94	74.08	57.98	21.88
3C90	74.92	62.44	28.77
A	81.92	64.30	38.61
B	70.31	55.47	7.69
C	77.77	58.03	25.79
D	140.20	137.49	35.62
E	121.98	145.31	24.57

Material	Waveshape	iGSE Error [%]	Hybrid Model Error [%]
N87	Sinusoid	30.06	5.10
N87	Triangle	26.43	9.51
N87	Trapezoid	23.84	6.73
N49	Sinusoid	41.38	12.85
N49	Triangle	35.96	9.81
N49	Trapezoid	33.72	7.67
N30	Sinusoid	18.75	4.53
N30	Triangle	19.96	2.49
N30	Trapezoid	18.26	3.43
N27	Sinusoid	28.33	4.50
N27	Triangle	27.07	6.73
N27	Trapezoid	24.45	5.88
78	Sinusoid	27.46	3.32
78	Triangle	26.90	5.68
78	Trapezoid	23.65	5.18
77	Sinusoid	30.12	5.03
77	Triangle	27.37	6.23
77	Trapezoid	25.55	5.00
3F4	Sinusoid	37.29	4.82
3F4	Triangle	39.26	6.32
3F4	Trapezoid	33.80	5.16
3E6	Sinusoid	22.56	2.52
3E6	Triangle	29.56	2.23
3E6	Trapezoid	25.68	2.44
3C94	Sinusoid	28.30	4.62
3C94	Triangle	26.98	7.14
3C94	Trapezoid	24.61	6.06
3C90	Sinusoid	29.93	6.75
3C90	Triangle	27.88	9.22
3C90	Trapezoid	25.74	7.22
Material A	Sinusoid	39.16	26.86
Material A	Triangle	33.82	13.49
Material A	Trapezoid	28.72	9.69
Material B	Sinusoid	23.43	4.41
Material B	Triangle	23.79	2.68
Material B	Trapezoid	23.57	2.52
Material C	Sinusoid	31.84	17.16
Material C	Triangle	22.81	8.15
Material C	Trapezoid	19.75	6.67
Material D	Sinusoid	36.11	10.89
Material D	Triangle	40.96	12.59
Material D	Trapezoid	21.07	14.79
Material E	Sinusoid	18.26	9.79
Material E	Triangle	44.72	8.38
Material E	Trapezoid	35.66	6.74

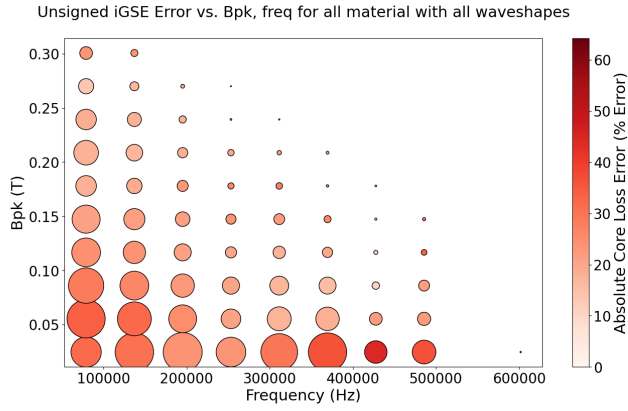


Figure 4: An error heatmap of the iGSE core loss model shows percent error on a color scale presented on an axis of peak flux density and frequency. The size of the point indicates the ratio of samples at that operating condition.

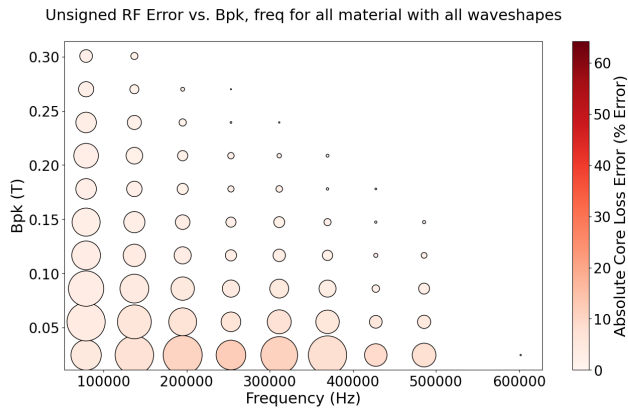


Figure 5: An error heatmap of the hybrid core loss model shows percent error on a color scale presented on an axis of peak flux density and frequency. The size of the point indicates the ratio of samples at that operating condition. The color scale shown is the same as in Figure 4 to offer a direct comparison.

### C. Limitations and Future Work

The flux-density waveform for all the data used to train the hybrid model presented in this paper has a DC bias of zero. Therefore, future areas of exploration may include the incorporation of DC bias into the model (shown to alter core loss in [11], [12]). Further improvements in accuracy can also be gained by including permeability as a feature if it is known for each material.

In practice, the proposed hybrid core-loss model can be used independently, simply to improve core-loss predictions in the context of the design of magnetic components. Other applications of this model include the incorporation into a larger data-driven design tool such as that described in [13].

### V. CONCLUSIONS

Equation-based approximations for modeling of core loss, such as [2], [3] have been widely used in power electronics practice. However, due to the wide range of desired operating conditions and irregularities in core materials, a more accurate model is necessary to improve core-loss modeling and truly enable optimization of magnetic components in switched-mode power converters. Taking advantage of the large database

of experimentally measured core loss samples in [1], this report presents a novel hybrid model that integrates the iGSE method [3] with a waveform classifier and a relatively simple machine-learning based, random forest regression to improve the modeling of core losses across operating conditions. The hybrid model is shown to reduce absolute percent error by a factor of four across all materials using only simple and easily available features. This approach eliminates the necessity for overly complex and computationally expensive methods such as neural networks while still offering greatly improved and repeatable results.

The model has significant potential to serve as an effective general model for core loss. Its performance on new materials will be shown in an upcoming paper at IEEE APEC 2024 [8].

### REFERENCES

- [1] H. Li, D. Serrano, T. Guillod, E. Dogariu, A. Nadler, S. Wang, M. Luo, V. Bansal, Y. Chen, C. R. Sullivan, and M. Chen, "MagNet: An Open-Source Database for Data-Driven Magnetic Core Loss Modeling," in *2022 IEEE Applied Power Electronics Conference and Exposition (APEC)*, 2022, pp. 588–595.
- [2] C. Steinmetz, "On the law of hysteresis," *Proceedings of the IEEE*, vol. 72, no. 2, pp. 197–221, 1984.
- [3] K. Venkatachalam, C. Sullivan, T. Abdallah, and H. Tacca, "Accurate prediction of ferrite core loss with nonsinusoidal waveforms using only Steinmetz parameters," in *2002 IEEE Workshop on Computers in Power Electronics*, 2002. *Proceedings.*, 2002, pp. 36–41.
- [4] X. Shen, H. Wouters, and W. Martinez, "Deep Neural Network for Magnetic Core Loss Estimation using the MagNet Experimental Database," in *2022 24th European Conference on Power Electronics and Applications (EPE'22 ECCE Europe)*, 2022, pp. 1–8.
- [5] E. Dogariu, H. Li, D. Serrano López, S. Wang, M. Luo, and M. Chen, "Transfer Learning Methods for Magnetic Core Loss Modeling," in *2021 IEEE 22nd Workshop on Control and Modelling of Power Electronics (COMPEL)*, 2021, pp. 1–6.
- [6] H. Li, S. R. Lee, M. Luo, C. R. Sullivan, Y. Chen, and M. Chen, "MagNet: A Machine Learning Framework for Magnetic Core Loss Modeling," in *2020 IEEE 21st Workshop on Control and Modeling for Power Electronics (COMPEL)*, 2020, pp. 1–8.
- [7] J. K. Jaiswal and R. Samikannu, "Application of Random Forest Algorithm on Feature Subset Selection and Classification and Regression," in *2017 World Congress on Computing and Communication Technologies (WCCCT)*, 2017, pp. 65–68.
- [8] B. Sauter, S. Reese, S. Sinha, J. Haddon, T. Byrd, and D. Maksimovic, "Integrating Equation-Based Methods with Random Forest Regression for Improved Accuracy of Magnetic Core Loss Modeling," in *2024 IEEE Applied Power Electronics Conference and Exposition (APEC)*, 2024.
- [9] F. Pedregosa, G. Varoquaux, A. Gramfort, V. Michel, B. Thirion, O. Grisel, M. Blondel, P. Prettenhofer, R. Weiss, V. Dubourg, J. Vanderplas, A. Passos, D. Cournapeau, M. Brucher, M. Perrot, and E. Duchesnay, "Scikit-learn: Machine Learning in Python," *Journal of Machine Learning Research*, vol. 12, pp. 2825–2830, 2011.
- [10] L. Breiman, "Random Forests," *Machine Learning*, vol. 45, no. 1, pp. 5–32, Oct 2001. [Online]. Available: <https://doi.org/10.1023/A:1010933404324>
- [11] J. Muhlethaler, J. Biela, J. W. Kolar, and A. Ecklebe, "Core Losses Under the DC Bias Condition Based on Steinmetz Parameters," *IEEE Transactions on Power Electronics*, vol. 27, no. 2, pp. 953–963, 2012.
- [12] B. N. Sanusi, M. Zambach, C. Frandsen, M. Beleggia, A. Michael Jørgensen, and Z. Ouyang, "Investigation and Modeling of DC Bias Impact on Core Losses at High Frequency," *IEEE Transactions on Power Electronics*, vol. 38, no. 6, pp. 7444–7458, 2023.
- [13] S. Reese, B. Sauter, S. Khandelwal, A. Kamalapur, T. Byrd, J. Haddon, and D. Maksimovic, "Loss estimation and design of dc-dc converters using physics- and data-based component models," in *2023 IEEE Applied Power Electronics Conference and Exposition (APEC)*, 2023, pp. 82–89.